

AICHE Annual Meeting
Miami Beach, Florida, November 1986
Session 10b4: Recent Advances in Process Control - II, Paper 74a
Chairman: K. McDonald

CONTROL OF ILL-CONDITIONED PLANTS: HIGH PURITY DISTILLATION

Sigurd Skogestad

Manfred Morari

Chemical Engineering, 206-41
California Institute of Technology
Pasadena, CA 91125
(818)356-4186

Abstract

High purity distillation columns are inherently ill-conditioned because the product compositions are very sensitive to changes in the product flow rates. This may cause performance problems if the uncertainty changes the directionality of the plant. This is the case for the traditional LV-configuration, where input uncertainty on the manipulated variables changes the directionality at the input of the plant, and makes it impossible to use an inverse based controller ("decoupler"). For the DV-configuration (direct material balance) the input uncertainty poses no problem. The structured singular value, μ , is used as a tool to study the effect of uncertainty on stability and performance in a systematic manner. Finally, large elements in the RGA are found to imply poor performance when there is input uncertainty.

I. INTRODUCTION

It is well known that ill-conditioned plants cause control problems (Morari and Doyle, 1986, Skogestad and Morari, 1985). By ill-conditioned we mean that the gain of the plant is strongly dependent on the input direction, or equivalently that the plant has a high condition number

$$\gamma(G(j\omega)) = \bar{\sigma}(G(j\omega)) / \underline{\sigma}(G(j\omega)) \quad (1)$$

Here $\bar{\sigma}(G)$ and $\underline{\sigma}(G)$ denote the maximum and minimum singular values of the plant

$$\bar{\sigma}(G) = \max_{u \neq 0} \frac{\|Gu\|}{\|u\|_2}$$

$$\underline{\sigma}(G) = \min_{u \neq 0} \frac{\|Gu\|}{\|u\|_2}$$

$\|\cdot\|_2$ denotes the usual Euclidian norm. We also say that an ill-conditioned plant is characterized by strong "directionality" because inputs in directions corresponding to high plant gains are strongly amplified in the plant, while inputs in directions corresponding to low plant gains are not.

The main reason for the control problems associated with ill-conditioned plants is "uncertainty". Uncertainty in the plant model may have several origins:

1. There are always parameters in the linear model which are known only approximately. For the distillation column such parameters may be the relative volatility or the number of theoretical stages.
2. Measurement devices have imperfections. This may give rise to uncertainty on the manipulated inputs in a distillation column, since they are usually measured and adjusted in a cascade manner.
3. At high frequencies even the structure and the model order is unknown, and the uncertainty will exceed 100% at some frequency.
4. The parameters in the linear model may vary due to nonlinearities or

changes in the operating conditions. Examples of this are given in Section V.

For "tight control" of ill-conditioned plants the controller has to compensate for the strong directionality by applying large input signals in the directions where the plant gain is low, that is, a controller similar to G^{-1} in directionality is desirable. However, because of uncertainty, the direction of the large input may not correspond exactly to the low gain in the plant and the amplification of these large input signals may be much larger than expected from the model. This will result in large values of the controlled variables y (Fig. 1), leading to poor performance or even instability.

The concept of directionality is clearly unique to multivariable systems, and extensions of design methods developed for SISO systems are likely to fail for multivariable plants with a high degree of directionality. Furthermore, since the problems with ill-conditioned plants are closely related to how the uncertainty affects the particular plant, it is very important to model the uncertainty as precisely as possible. Most multivariable design methods (LQG, LQG/LTR, INA/DNA, IMC, etc.) do not explicitly take the uncertainty description into account, and these methods will in general not give acceptable designs for ill-conditioned plants.

A distillation column will be used as an example of an ill-conditioned plant. Here the product compositions are very sensitive to changes in the external flows (high gain in this direction), but quite insensitive to changes in the internal flows (low gain in this direction). Distillation columns are a major consumer of energy in the chemical industry, and there is a large potential for savings by maintaining tighter control of the product compositions. One interesting property of distillation columns is that the

condition number may be arbitrary large if the purity of the products is sufficiently high. In this paper the main emphasis is on general properties of ill-conditioned plants, rather than on the control system design for a real distillation column.

II. DISTILLATION COLUMN EXAMPLE

Fundamentals of Distillation Control

The objective of a distillation column (Fig. 2) is to split the feed, F , which is a mixture of a light and a heavy component, into a distillate product, D , which contains most of the light component, and a bottom product, B , which contains most of the heavy component. The compositions z_F , y_D and x_B of these streams refer to the mole fractions of light component. Perfect separation would be obtained with $y_D = 1$ and $x_B = 0$. The driving force for this separation is the difference in volatility between the heavy (H) and light (L) component, which can be expressed by the relative volatility

$$\alpha = \frac{y_L/x_L}{y_H/x_H}$$

- x - mole fraction in liquid
- y - mole fraction in vapor in equilibrium with x

For a binary separation $y_H = 1 - y_L$ and $x_H = 1 - x_L$, and we get

$$y = \frac{\alpha x}{1 + (\alpha - 1)x} \quad (2)$$

(the subscript L is generally dropped for the light component). In a distillation column separation is improved over what can be obtained with one stage (Eq. 2), by stacking stages on top of each other as shown in Fig. 2. In such a distillation column there are five controlled variables

- Vapor holdup (expressed by the pressure p)

manipulated variables for composition control, i.e.,

$$y = \begin{bmatrix} \Delta y_D \\ \Delta x_B \end{bmatrix}, \quad u = \begin{bmatrix} \Delta L \\ \Delta V \end{bmatrix}$$

This choice is often made since L and V have an immediate effect on the product compositions y_D and x_B , respectively. By linearizing the steady state model and assuming that the dynamics may be approximated by a first order response with time constant $\tau = 75$ min, we derive the following linear model

$$\begin{bmatrix} dy_D \\ dx_D \end{bmatrix} = G_{LV} \begin{bmatrix} dL \\ dV \end{bmatrix}, \quad G_{LV} = \frac{1}{\tau s + 1} \begin{bmatrix} 0.878 & -0.864 \\ 1.082 & -1.096 \end{bmatrix} \quad (3)$$

This is admittedly a very crude model of this strongly nonlinear plant, but the model is simple and displays the main features of the distillation column behavior. The use of a low order model for this high order plant turns out to be a good approximation, since one time constant is usually dominating (Moczek, et al., 1965). In Section V we will consider the nonlinearities in more detail, and discuss how these may be treated as uncertainty on the linear model (3).

Singular Value Analysis of the Model

The condition number of the plant (3) is

$$\gamma(G_{LV}) = 141.7$$

and the 1-1 element of the RGA is

$$\lambda_{LV} = \left(1 - \frac{1.082 \cdot 0.864}{0.878 \cdot 1.096}\right)^{-1} = 35.1$$

which shows a high degree of directionality in the plant. More specific information about this directionality is obtained from the Singular Value Decomposition (SVD) of the steady state gain matrix

$$G = U \Sigma V^H$$

or equivalently since $V^H = V^{-1}$

- Liquid holdup in accumulator (M_D)
- Liquid holdup in column base (M_B)
- Top composition (y_D)
- Bottom composition (x_B)

and five manipulated inputs

- Distillate flow (D)
- Bottom flow (B)
- Reflux (L)
- Boilup (V) (controlled indirectly by the reboiler duty)
- Overhead vapor (V_t) (controlled indirectly by the condenser duty)

Because the composition dynamics are usually much slower than the flow dynamics, we will make the simplifying assumption of perfect control of holdup (i.e., p , M_D , M_B constant) and instantaneous flow responses. With these assumptions and using the mole fractions of the light component at each stage as state variables, we easily derive the nonlinear model shown in the Appendix. Different control configurations are obtained by choosing different inputs pairs (e.g., L and V) for composition control; the remaining three manipulated inputs are then determined by the requirement of keeping p , M_D and M_B under perfect control. Irrespective of the control configuration, the two operating variables corresponding to the high and low plant gain are, as we shall see, the external flows (product flow rates, D and B) and the internal flows (which are changed by changing the reflux L and boilup V while keeping D and B constant).

Model of the Distillation Column

The distillation column described in Table $\frac{1}{2}$ will be used as an example. The overhead composition is to be controlled at $y_D = 0.99$ and the bottom composition at $x_B = 0.01$. Consider first using reflux L and boilup V as

$$G\bar{v} = \bar{\sigma}(G)\bar{u}$$

$$G\underline{v} = \underline{\sigma}(G)\underline{u}$$

where

$$\Sigma = \text{diag}(\bar{\sigma}, \underline{\sigma}) = \text{diag}(1.972, 0.0139)$$

$$V = [\bar{v} \quad \underline{v}] = \begin{bmatrix} 0.707 & 0.708 \\ -0.708 & 0.707 \end{bmatrix} \quad U = [\bar{u} \quad \underline{u}] = \begin{bmatrix} 0.625 & 0.781 \\ 0.781 & -0.625 \end{bmatrix}$$

The large plant gain, $\bar{\sigma}(G) = 1.972$, is obtained when the inputs are in the direction $\begin{bmatrix} dL \\ dV \end{bmatrix} = \bar{v} = \begin{bmatrix} 0.707 \\ -0.708 \end{bmatrix}$. Since

$$dB = -dD = dL - dV \quad (4)$$

this physically corresponds to the direction with the largest change in the external flows, D and B. From the direction of the output vector $\bar{u} = \begin{bmatrix} 0.625 \\ 0.781 \end{bmatrix}$, we see that changes in the external flows move the outputs in the same direction, i.e., mainly affect the average composition $\frac{y_D + x_B}{2}$.

Any column with products of high purity is sensitive to changes in the external flows because the distillate rate D has to be about equal to the amount of light component in the feed. Any imbalance leads to large changes in the product compositions. Assume in our example that the distillate flow D is increased by 5% to 0.525 kmol/min. Since there is only 0.5 kmol/min of light component in the feed at least 0.025 kmol/min of this has to be heavy component. The best attainable value for the top composition, even with total reflux, is then $y_D = 0.5/0.525 = 0.952$. This is far from the desired $y_D = 0.99$.

The low plant gain, $\underline{\sigma}(G) = 0.0139$, is obtained for inputs in the direction

$$\begin{bmatrix} dL \\ dV \end{bmatrix} = \underline{v} = \begin{bmatrix} 0.708 \\ 0.707 \end{bmatrix}. \quad \text{From (4) observe that physically this corresponds to}$$

changing the internal flow only ($dB = dD \approx 0$), and from the output vector $\underline{u} =$

$\begin{bmatrix} 0.781 \\ -0.625 \end{bmatrix}$, we see that the effect is to move the outputs in different directions, i.e., to change $y_d - x_B$. Thus, it takes a large control action to move the compositions in different directions and to make both products purer simultaneously.

The notion that some changes are more "difficult" than others is important, since it implies that some disturbances may be "easier" to reject than others. Let d be the effect of the disturbance on the outputs (Fig. 1), or let d represent a setpoint change. A disturbance d which has a direction close to \bar{u} , is expected to be "easy" to reject since it corresponds to the high plant gain. Similarly, a disturbance close to \underline{u} in direction is expected to be more difficult. The disturbance condition number, $\gamma_d(G)$, gives a more precise measure of how the disturbance is "aligned" with the directions of the plant (Skogestad and Morari, 1986a).

$$\gamma_d(G) = \frac{\|G^{-1}d\|_2}{\|d\|_2} \bar{\sigma}(G) \quad (5)$$

$\gamma_d(G)$ ranges in value between 1 and $\gamma(G)$. A value close to 1 indicates that the disturbance is in the "good" direction (\bar{u}) corresponding to the high plant gain, $\bar{\sigma}(G)$. A value close to $\gamma(G)$ indicates that the disturbance is in the "bad" direction (\underline{u}) corresponding to the low plant gain, $\underline{\sigma}(G)$. We will consider the following two disturbances (actually setpoint changes) in the simulations

$$y_{S_1} = \begin{bmatrix} 1 \\ 0 \end{bmatrix} \quad \text{with} \quad \gamma_{d_1}(G) = 110.5$$

$$y_{S_2} = \begin{bmatrix} 0.4 \\ 0.6 \end{bmatrix} \quad \text{with} \quad \gamma_{d_2}(G) = 12.3$$

y_{S_1} corresponds to a setpoint change in y_D only, and is seen to be a change with a large component in the "bad" direction. The direction of y_{S_2}

corresponds to that of a feed flow rate disturbance (Table 1) and it is seen to have a large component in the "good" direction corresponding to the high plant gain.

Linear Closed Loop Simulations

Linear simulations of the distillation column using the model (3) will now be used to support the following three claims regarding ill-conditioned plants:

1. Inverse-based controllers are potentially very sensitive to uncertainty on the input variables.
2. Low condition-number controllers are less sensitive to uncertainty, but the response is strongly dependent on the direction of the disturbance.
3. ~~Changing the plant may make the plant~~ ^{Not all ill-conditioned plants are} insensitive to uncertainty on the input variables.

1. Inverse-based controllers are potentially very sensitive to uncertainty on the input variables

The inverse-based controller

$$C_1(s) = \frac{k_1}{s} G_{LV}^{-1}(s) = \frac{k_1(1+75s)}{s} \begin{bmatrix} 39.942 & 31.487 \\ 39.432 & -31.997 \end{bmatrix}, k_1 = 0.7 \text{ min}^{-1} \quad (6)$$

may be derived by using the IMC design procedure with a first order filter or by using a steady state decoupler plus a PI controller. This controller should in theory remove all the directionality of the plant and give rise to a decoupled first order response with time constant 1.43 min. This is indeed confirmed by the simulations in Fig. 3A and Fig. 4A for the case with no uncertainty. In practice, the plant behavior will be different from the model, and for the simulations in Fig. 3B and 4B an error of 20% in the change of each of the manipulated inputs is assumed:

$$dL = 1.2 dL_c, dV = 0.8 dV_c \quad (7)$$

(dL and dV are the actual changes in the manipulated flow rates, while dL_c and dV_c are the desired values as computed by the controller). It is important to stress that this kind of diagonal input uncertainty, which stems from the inability to know the exact values of the manipulated variables, is always present, although the actual size of the uncertainty may vary. For the setpoint change in y_D (Fig. 3B) the simulated response with uncertainty differs drastically from the one predicted by the model, and the response is clearly not acceptable. The response is no longer decoupled, and Δy_D and Δx_B reach a value of about 6 before settling at their desired values of 1 and 0. The uncertainty has less deteriorating effect for the feed rate "disturbance" (Fig. 4B) which occurs mostly in the "good" direction.

There is a simple physical explanation for the observed poor response to the setpoint change in y_D . To accomplish this change, which occurs mostly in the "bad" direction corresponding to the low plant gains, the inverse-based controller generates a large change in internal flows ($dL + dV$), while trying to keep the changes in the external flows ($dB = -dD = dL - dV$) very small. However, uncertainty with respect to the values of dL and dV makes it impossible to keep $dL - dV$ small and the consequence is large changes in the ~~internal~~^{external} flows. This results in large changes in the compositions because of the high plant gain in this direction. This particular problem may be avoided by controlling D or B directly as will be shown below.

A more mathematical way of showing how the uncertainty changes the plant is as follows: Let the plant transfer model be $G(s)$ and assume there is uncertainty with respect to each of the manipulated variables, i.e., the actual ("perturbed") plant is

$$G_p = G(I+\Delta) , \Delta = \begin{bmatrix} \Delta_1 & 0 \\ 0 & \Delta_2 \end{bmatrix}$$

where Δ_1 and Δ_2 represent the relative uncertainty for each input. With an inverse based controller, $C(s) = c(s)G(s)^{-1}$, the loop transfer matrix becomes

$$G_p C = c(s)G(I+\Delta)G^{-1} = c(s)(I+G\Delta G^{-1}) \quad (8)$$

The error term

$$G_{LV}\Delta G_{LV}^{-1} = \begin{bmatrix} 35.1 \Delta_1 - 34.1 \Delta_2 & -27.7 \Delta_1 + 27.7 \Delta_2 \\ 43.2 \Delta_1 - 43.2 \Delta_2 & -34.1 \Delta_1 + 35.1 \Delta_2 \end{bmatrix} \quad (9)$$

is worst when Δ_1 and Δ_2 have different signs. With $\Delta_1 = 0.2$ and $\Delta_2 = -0.2$ (as used in the simulations, Eq. (7)) we find

$$G_{LV}\Delta G_{LV}^{-1} = \begin{bmatrix} 13.8 & -11.1 \\ 17.2 & -13.8 \end{bmatrix}$$

The elements in this matrix are much larger than one, and the observed poor response is not surprising.

2. Low condition number controllers are less sensitive to uncertainty, but the response is strongly dependent on the direction of the disturbance.

The poor response for the case with uncertainty in the example above was caused by the high condition-number controller which generates large input signals in the directions corresponding to the small plant gain. The simplest way to make the closed loop system less sensitive to the input uncertainty is to use a low condition number controller which does not have large gains in any particular direction. The problem with such a controller is that little or no correction is made for the strong directionality of the plant. This results in a closed loop response which depends strongly on the disturbance direction, as shown below. The diagonal controller

$$C_2(s) = \frac{k_2(75s+1)}{s} \begin{bmatrix} 1 & 0 \\ 0 & -1 \end{bmatrix} , k_2 = 2.4 \text{ min}^{-1} \quad (10)$$

consists of two equal single loop PI controllers and has a condition number of one. As seen from the simulations in Fig. 5 and 6 the quality of the closed loop response depends strongly on the disturbance direction, but is only weakly influenced by uncertainty. The response to y_{S_1} is very sluggish, while the response to y_{S_2} is fast initially, but approaches the final steady state sluggishly. Note that a disturbance in the "good" direction

$$y_S = \underline{u} = \begin{bmatrix} 0.625 \\ 0.781 \end{bmatrix} \quad \text{with} \quad \gamma_d(G)=1$$

generates a first order nominal response with time constant $1/2.4 \cdot \bar{\sigma}(G) = 0.21$ min. A disturbance in the "bad" direction

$$y_S = \underline{u} = \begin{bmatrix} 0.781 \\ -0.625 \end{bmatrix} \quad \text{with} \quad \gamma_d(G)=141.7$$

generates a first order nominal response with time constant $1/2.4 \cdot \underline{\sigma}(G) = 30$ min. All other responses are linear combinations of these two extremes (Fig.5A and 6A).

3. ~~Not all 20 conditions think are~~
~~Changing the plant may make the system insensitive to uncertainty on the~~
input variables

We already argued physically that the plant might be made less sensitive to uncertainty by controlling the external flows directly. Consider the case of distillate flow D and boilup V as manipulated variables ("direct material balance control") (Shinskey, 1984). Assuming perfect level and pressure control, i.e., $dL = dV - dD$, we have

$$\begin{bmatrix} dL \\ dV \end{bmatrix} = \begin{bmatrix} -1 & 1 \\ 0 & 1 \end{bmatrix} \begin{bmatrix} dD \\ dV \end{bmatrix} \quad (11)$$

and the following linear model is derived from (3)

$$\begin{bmatrix} dy_D \\ dx_B \end{bmatrix} = G_{DV} \begin{bmatrix} dD \\ dV \end{bmatrix}$$

$$G_{DV} = G_{LV} \begin{bmatrix} -1 & 1 \\ 0 & 1 \end{bmatrix} = \frac{1}{1+75s} \begin{bmatrix} -0.878 & 0.014 \\ -1.082 & -0.014 \end{bmatrix} \quad (12)$$

In practice the condenser level loop introduces a lag between the change in distillate flow, dD , and the reflux flow, dL (which is the input which actually affects the compositions), but this is neglected here. It is important to note that with (11) and without input uncertainty, identical responses may be obtained with the LV-plant (3) and the DV-plant (12) by using multivariable controllers. The plant (12) is also ill-conditioned

$$\gamma(G_{DV}) = 70.8, \quad \lambda_{DV} = \frac{0.448}{0.5}$$

In this case the SVD yields

$$\Sigma = \begin{bmatrix} 1.393 & 0 \\ 0 & 0.0197 \end{bmatrix}, \quad V = \begin{bmatrix} -1.000 & -0.001 \\ -0.001 & 1.000 \end{bmatrix}, \quad U = \begin{bmatrix} 0.630 & 0.777 \\ 0.777 & -0.630 \end{bmatrix}$$

The high gain corresponds to an input $\begin{bmatrix} dD \\ dV \end{bmatrix}$ in the direction of $\bar{v}(G_{DV}) =$

$$\begin{bmatrix} -1.000 \\ -0.001 \end{bmatrix}, \text{ which, as expected, corresponds to a change in the external flows.}$$

The low gain again corresponds to a change in the internal flows ($dD \approx 0$). Note that in this case there is one manipulated variable (dD) which acts in the high gain, and one (dV) which acts in the low gain direction. This "decomposition" is significant, since uncertainty in dV , does not affect the external flows, dD .

The value of the RGA of $\frac{0.45}{0.5}$ suggests that the system may be difficult to control using decentralized control, but also suggests a plant which is not sensitive to uncertainty (Grosdidier, 1986). To confirm that the system is much less sensitive to uncertainty in this case, consider the following inverse-based controller

$$C_3(s) = \frac{k_3}{s} G_{DV}(s)^{-1} = \frac{k_3(1+75s)}{s} \begin{bmatrix} -0.5102 & -0.5102 \\ 39.43 & -32.00 \end{bmatrix}, \quad k_3 = 0.7 \text{ min}^{-1} \quad (13)$$

Without uncertainty this controller gives the same response as controller $C_1(s)$

with the LV-configuration. However, in this case the decoupled first order response with time constant 1.43 min is maintained also when there is uncertainty on the manipulated variables (Fig. 7 and 8). The following error with respect to dD and dV was used

$$dD = 1.2 dD_C, dV = 0.8 dV_C \quad (14)$$

From this example we see that ill-conditioned plants by themselves may not give performance problems if the uncertainty is appropriately aligned with the process. For the DV-configuration we find the error matrix $G\Delta G^{-1}$ (8)

$$G_{DV\Delta G}^{-1} = \begin{bmatrix} 0.45 \Delta_1 + 0.55 \Delta_2 & 0.45 \Delta_1 - 0.45 \Delta_2 \\ -0.55 \Delta_1 + 0.55 \Delta_2 & 0.55 \Delta_1 + 0.45 \Delta_2 \end{bmatrix}$$

and with $\Delta_1 = 0.2$ and $\Delta_2 = -0.2$ corresponding to (14)

$$G_{DV\Delta G}^{-1} = \begin{bmatrix} -0.02 & 0.18 \\ -0.22 & 0.02 \end{bmatrix}$$

The elements in this matrix are small compared to one, and good performance is maintained even in the presence of uncertainty on each input. The nonzero off-diagonal elements explain why the response in Fig. 7B is not completely decoupled.

III. ROBUSTNESS ANALYSIS WITH μ

It is quite evident from the linear simulations above that multivariable systems exhibit a type of "directionality" which may make the closed loop response strongly dependent on the particular disturbance and model error assumed. One of the major weaknesses with the simulation approach is that it may be very difficult and time-consuming to find by trial-and-error the particular disturbance and model error which causes control problems. Therefore there is a need for a tool which solves the following robust performance problem in a more systematic manner:

Given a nominal plant, an uncertainty description, a set of possible disturbances and setpoint changes, a desired performance objective, and a controller: Will the "worst case" response satisfy the desired performance objectives?

If performance (allowed size of input and output signals) is defined using the H^∞ -norm and the uncertainty is described in terms of norm bounds in the frequency domain, this problem is solved fairly easily by computing Structured Singular Value μ (Doyle, 1982) of a particular matrix N at each frequency (Doyle, 1985). The elements in the matrix N are determined by the nominal model, the size and nature of the uncertainty, and the performance specifications. Robust performance is guaranteed if and only if $\mu(N) < 1$ for all frequencies.

Some Definitions

Let us make a pause to define some of the terms used above more carefully. Achieving robust performance is clearly the ultimate goal of the controller design. However, it may be easier to solve this problem by first considering some subobjectives which have to be satisfied in order to achieve this:

Nominal Stability (NS): The model is assumed to be a reasonable approximation of the true plant. Therefore the closed loop system with the controller applied to the (nominal) plant model has to be stable.

Nominal Performance (NP): In addition to stability, the quality of the response should satisfy some minimum requirements - at least when the controller is applied to the plant model. For mathematical convenience we will define performance in terms of the weighted H^∞ -norm of the closed-loop transfer function between external inputs (disturbances and setpoints) and

"errors" (may include $y_D - y_{D_S}$, $x_B - x_{B_S}$, manipulated inputs u , etc.). The simplest example of such a performance specification is a bound on the weighted sensitivity function

$$\bar{\sigma}(W_{1P} S W_{2P}) \leq 1 \quad \forall \omega, S = (I + GC)^{-1} \quad (16a)$$

The input weight W_{2P} is often equal to the disturbance model. The output weight W_{1P} is used to specify the frequency range over which the errors are to be small and (if W_{1P} is not equal to $w_p(s)I$) which outputs are more important.

Robust Stability (RS): The closed loop system must remain stable for all possible plants as defined by the uncertainty description.

Robust Performance (RP): The closed loop system must satisfy the performance requirements for all possible plants as defined by the uncertainty description. As an example we may require (16a) to be satisfied when G is replaced by any of the possible perturbed plants G_p as defined by the uncertainty description.

$$\bar{\sigma}(W_{1P}(I + G_p C)^{-1} W_{2P}) \leq 1 \quad \forall \omega, \forall G_p \quad (16b)$$

Most controller design methods (even "modern" optimal control, LQG), only address the problems of Nominal Stability and Nominal Performance. The stability margins in the classical frequency domain design methods, are an attempt to address the Robust Stability problem, but these margins may be misleading and are a very indirect method.

Conditions for Robust Stability and Robust Performance

The definition of Robust Performance given above is of no value without simple methods to test if conditions like (16b) are satisfied for all possible perturbed plants G_p . Below we will state computationally useful conditions for RS and RP using the Structured Singular Value μ for the case when the uncertainty (the possible plants G_p) is modelled in terms of a set of norm-

bounded perturbations on the nominal system. By use of weights each perturbation is normalized to be of size one:

$$\bar{\sigma}(\Delta_i) \leq 1 \quad \forall \omega$$

The perturbations, which may occur at different locations in the system, are collected in the diagonal matrix Δ

$$\Delta = \text{diag}\{\Delta_1, \dots, \Delta_n\}$$

and the system is rearranged to match the structure in Fig. 9. We will not go into detail on how this is done at this point. This will become clearer by studying the distillation column example in Section IV and V. The signal \hat{d} in Fig. 9 represents the external inputs (weighted disturbances and setpoint changes) affecting the system. The signal \hat{e} represents the weighted errors, or more generally the signals which are to be kept "small". The interconnection matrix N in Fig. 9 is a function of the nominal plant G , the controller C and the uncertainty weights. Performance weights are also absorbed into N such that the performance specifications involving \hat{e} and \hat{d} are normalized:

Robust Performance Specification: (Fig. 9)

$$\bar{\sigma}(E) \leq 1 \quad \forall \omega, \forall \Delta \quad (17)$$

$$\text{where } \hat{e} = E\hat{d}, E = N_{22} + N_{21}\Delta(I - N_{11}\Delta)^{-1}N_{12}$$

An example of such a performance specification is Eq. (16b). With these assumptions for the uncertainty and performance we have the following results (Doyle, 1985).

$$\text{N.S.} \Leftrightarrow N \text{ stable (internally)} \quad (18)$$

$$\text{N.P.} \Leftrightarrow \mu_{\text{NP}} = \sup_{\omega} \bar{\sigma}(N_{22}) < 1 \quad (19)$$

$$\text{R.S.} \Leftrightarrow \mu_{\text{RS}} = \sup_{\omega} \mu_{\Delta}(N_{11}) < 1 \quad (20)$$

$$\text{R.P.} \Leftrightarrow \mu_{\text{RP}} = \sup_{\omega} \mu(\Delta_{\Delta P})(N) < 1 \quad (21)$$

The quantities μ_{NP} , μ_{RS} and μ_{RP} represent the " μ -norms" and are introduced as a convenient notation. The conditions for N.P. and R.S. are necessary in order to satisfy the R.P. condition. Note that $\mu_{\Delta}(N_{11})$ is a function of both the matrix N_{11} and the structure of the uncertainty Δ . The Robust Performance condition (21) is computed with respect to the structure $\text{diag}(\Delta, \Delta_P)$, where Δ_P is a full matrix of the same size as N_{22} . The use of μ is less conservative than using any other matrix norm. In particular,

$$\mu_{\Delta}(N) \leq \bar{\sigma}(N)$$

and the equality holds only when Δ is a full matrix. The use and implications of conditions (19)-(21) will hopefully become clearer by studying how these results apply to the distillation column example.

IV. μ -ANALYSIS OF THE DISTILLATION COLUMN

Problem Definition

To study Robust Stability and Robust Performance of the distillation column using μ , the uncertainty and performance specifications must be defined. The same uncertainty and performance specifications will be assumed for the LV-configuration (3) and the DV-configuration (12). (In general, it is reasonable to use the same performance specifications, but the uncertainty may be different).

Uncertainty: The uncertainty with respect to the manipulated inputs which was discussed in Section II may be represented as multiplicative input uncertainty (Fig. 10)

$$G_D = G(I + w_I(s)\Delta_I), \quad \bar{\sigma}(\Delta_I) < 1 \quad \forall \omega \quad (22)$$

where $w_I(s)$ describes the magnitude of the relative uncertainty on each manipulated input

$$w_I(s) = 0.2 \frac{5s+1}{0.5s+1} \quad (23)$$

This implies an input error of up to 20% in the low frequency range as was assumed for the simulations. The uncertainty increases at high frequencies, reaching a value of one at about $\omega = 1 \text{ min}^{-1}$. The increase at high frequency may take care of the neglected flow dynamics. For the LV-configuration it allows for a time delay of about 1 minute in the responses between L and V and the outputs y_D and x_B . It may also represent neglected valve dynamics, dynamics for the heat transfer in the reboiler (for V), etc.

At first the uncertainty will be assumed to be unstructured, i.e., the perturbation matrix Δ_I is a full 2x2 matrix. This does not make much sense from a physical point of view, but is done for mathematical convenience. It will turn out that this assumption does not make any difference for the LV-configuration. The set of possible plants is now generated from Eq. (22) by allowing any 2x2 matrix Δ_I which satisfies $\bar{\sigma}(\Delta_I) \leq 1, \forall \omega$.

Performance: We will consider the simple case with

$$y_S = \begin{bmatrix} \Delta y_{Ds} \\ \Delta x_{Bs} \end{bmatrix}$$

(setpoint changes in y_D and x_B) as external inputs and

$$e = y - y_S = \begin{bmatrix} y_D - y_{Ds} \\ x_B - x_{Bs} \end{bmatrix}$$

as errors. These signals are related through the sensitivity function

$$e = -S_p y_S, \quad S_p = (I + G_p C)^{-1}$$

y_S and e are related to the weighted external inputs (\hat{d}) and errors (\hat{e}) by

$$y_S = W_{2p} \hat{d}, \quad \hat{e} = W_{1p} e$$

and we have

$$\hat{e} = E \hat{d}, \quad E = -W_{1p} S_p W_{2p} \quad (24)$$

We choose to express the performance specifications through the weights

$$W_{2P} = I, W_{1P} = w_P I, w_P(s) = 0.5 \frac{10s+1}{10s} \quad (25)$$

The Robust Performance specification (17) then becomes

$$\bar{\sigma}(S_P) < 1/|w_P|, \forall \omega \quad (26)$$

This bound on the sensitivity function S_P should be satisfied for all allowable G_P given by (22). The performance weight $w_P(s)$ (25) implies that we require integral action ($w_P(0) = \infty$) and allow an amplification of disturbances at high frequencies of at most a factor of two ($\lim_{\omega \rightarrow \infty} |w_P(i\omega)|^{-1} = 2$). A particular sensitivity function which exactly matches the performance bound (26) at low frequencies and satisfies it easily at high frequencies is

$$S = \left(\frac{20s+1}{20s} \right)^{-1} I$$

This corresponds to a first order response with time constant 20 min.

Performance and Stability Conditions

With the information given above the matrix N in the ΔN -structure (Fig. 9) becomes

$$N = \begin{bmatrix} -w_I C S G & w_I C S \\ w_P S G & -w_P S \end{bmatrix}, S = (I+GC)^{-1} \quad (27)$$

This matrix is found from Fig. 10 by assuming that the loops are "broken" ($\Delta_I=0$) at the input and output of the block Δ_I . As an example with $\Delta_I=0$, the transfer function from the external inputs ($\hat{d}=y_S$) to the errors ($\hat{e}=w_P(y-y_S)$) is

$$N_{22} = -w_P(I+GC)^{-1}$$

Similarly, the transfer function from \hat{d} to the input of Δ_I is

$$N_{12} = w_I C(I+GC)^{-1}$$

Conditions for Nominal Performance and Robust Stability are derived from (19) and (20) by using (27)

$$\text{N.P.} \quad \Leftrightarrow \quad \bar{\sigma}(S) \leq 1/|w_P| \quad \forall \omega, \quad S = (I+GC)^{-1} \quad (28)$$

$$\text{R.S.} \quad \Leftrightarrow \quad \bar{\sigma}(H_I) \leq 1/|w_I| \quad \forall \omega, \quad H_I = CG(I+GC)^{-1} = CSG \quad (29)$$

The condition for Robust Stability is expressed in terms of $\bar{\sigma}$ since Δ_I is assumed to be a full matrix. Note that S is the nominal sensitivity function at the output of the plant, while H_I is the closed loop transfer function as seen from the input of the plant. In some cases $GC = CG$ (in particular this is the case for the controllers $C_1(s)$, $C_2(s)$ and $C_3(s)$ in our examples) and we have

$$H_I = H, \quad H = GC(I+GC)^{-1} = I - S$$

where H is the closed loop transfer function as seen from the output of the plant. However, this will generally not be the case for multivariable systems.

The Robust Performance specification (26) should be satisfied for all plants given by (22). From (21) one finds

$$\text{R.P.} \quad \Leftrightarrow \quad \mu(\Delta_I \Delta_P)(N) \leq 1, \quad \forall \omega \quad (30)$$

Analysis of the LV-Configuration

The set of possible plants is given by (22) with $G = G_{LV}$ (3). We will analyze the LV-configuration for the inverse-based and the diagonal controller.

$$C_1(s) = c_1(s)G_{LV}^{-1}(s) \quad (31)$$

$$C_2(s) = c_2(s) \begin{bmatrix} 1 & 0 \\ 0 & -1 \end{bmatrix} \quad (32)$$

We will first consider the choices $c_1(s) = \frac{0.7}{s}$ and $c_2(s) = \frac{2.4(1+\tau s)}{s}$ used in the simulations in Section II, and then let

$$c_1(s) = \frac{k_1}{s}, \quad c_2(s) = \frac{k_2(1+\tau s)}{s} \quad (33)$$

and see if Robust Performance can be improved with other choices for k_1 and k_2 . Finally, we will consider the " μ -optimal" controller, $C_\mu(s)$, i.e., the

controller which minimizes μ_{RP} . We found this controller through a software package which uses a somewhat simplified version of the μ -synthesis procedure described by Doyle (1985). The simplification involves only considering the upper left corner when minimizing the H_∞ -norm of Eq. (7.3) in Doyle's paper (1985). This means that the resulting controller is not necessarily optimal.

Nominal Performance and Robust Stability. One way of designing controllers which meet the N.P. and R.S. specifications is to use multivariable loop shaping (Doyle and Stein, 1981). For Nominal Performance, $\underline{\sigma}(GC)$ must be above $|w_P|$ at low frequencies. For Robust Stability with input uncertainty, $\bar{\sigma}(CG)$ must lie below $1/|w_I|$ at high frequencies (Fig. 11).

For the inverse-based controller (31) we get $\bar{\sigma}(C_1G) = \underline{\sigma}(GC_1) = |c_1|$ and it is trivial to choose a $c_1(s)$ to satisfy these conditions. The choice $c_1(s) = \frac{0.7}{s}$ which was used in the simulations gives a controller which has much better nominal performance than required, and which can allow about two times more uncertainty than assumed. This is also seen from Fig. 12 and 13 where the Nominal Performance and Robust Stability conditions (28) and (29) are displayed graphically.

For the diagonal controller (32) we find $\bar{\sigma}(C_2G) = 1.972 |c_2|$ and $\underline{\sigma}(GC_2) = 0.0139 |c_2|$, and the difference between these two singular values is so large that no choice of c_2 is able to satisfy both N.P. and R.S. This is shown graphically in Fig. 12 and 13 for the choice $c_2(s) = \frac{2.4(1+75s)}{s}$.

Robust Performance. In the case with input uncertainty a sufficient ("conservative") test for Robust Performance in terms of singular values is (Doyle, 1986)

$$\text{R.P.} \quad \gamma \cdot \bar{\sigma}(w_P S) + \bar{\sigma}(w_I H_I) \leq 1 \quad \forall \omega \quad (34a)$$

$$\text{or } \text{R.P.} \leq \bar{\sigma}(w_p S) + \gamma \cdot \bar{\sigma}(w_I H_I) \leq 1 \quad \forall \omega \quad (34b)$$

Here γ denotes the condition number of the plant or the controller (the smallest one should be used). These conditions indicate that the use of an ill-conditioned controller ($\gamma(C_1)=141.7$) may give very poor Robust Performance even though both the Nominal Performance ($\bar{\sigma}(w_p S) < 1$) and Robust Stability conditions ($\bar{\sigma}(w_I H_I) < 1$) are individually satisfied. If a controller with a low condition number ($\gamma(C_2)=1$) is used we see that we get R.P. for "free" provided we have satisfied N.P. and R.S. This is always the case for SISO systems and gives a partial explanation for why Robust Performance was never an important issue in the classical control literature (Doyle, 1986).

Conditions (34) are very useful since they directly show how the Robust Performance condition is related to N.P. and R.S. and the condition number. However, (34) may be very conservative and in order to get a "tight" condition for R.P. the μ -condition (30) has to be used where N is given by (27). μ for R.P. is plotted in Fig. 14 and 15 for the two controllers $C_1(s)$ and $C_2(s)$ used in the simulations. As expected, the inverse-based controller $C_1(s)$ is far from meeting the Robust Performance requirements (μ_{RP} is about 5.8), even though the controller was shown to achieve both N.P. and R.S. On the other hand, the performance of the diagonal controller $C_2(s)$ is much less affected by uncertainty. ($\mu_{RP} = 1.71$).

Optimizing k_1 and k_2 wrt. R.P. For the inverse-based controller the "optimal" value for k_1 is 0.14 corresponding to a value of μ_{RP} equal to 3.3 which still

implies poor performance. This value for k_1 seems reasonable since it corresponds to a loop shape k_1/s which is further away from the R.S. constraint in Fig. 11.

For the PI-controller, the optimal gain is $k_2 = 2.4$, which is the value already used ($\mu_{RP} = 1.70$). It is not clear how low μ_{RP} can be made if $C(s)$ is only restricted to be diagonal (decentralized control); we were able to get μ_{RP} down to 1.42 by a trial-and-error procedure.

μ -Optimal Controller. The synthesis method (Doyle, 1985) used to design the " μ -optimal" controller gives controllers of very high order, but by employing model reduction, we were able to find a " μ -optimal" controller with 6 states. μ for R.P. for this controller is shown as a function of frequency in Fig. 16. (The μ -plot is not quite flat as it should be for the optimal case). The peak value for μ is 1.06, which means that this controller "almost" satisfies the Robust Performance condition. This value for μ_{RP} is significantly lower than for the diagonal PI controller, $C_2(s)$, and the time responses are also better as shown in Fig. 16 and 17. In particular, the approach to steady state is much faster. The state space realization of this μ -optimal controller is shown in Fig. 18. At low frequencies the controller is approximately

$$C_\mu(s) \approx \frac{(1+75s)}{s} \begin{bmatrix} 3.82 & -0.92 \\ 1.73 & -3.52 \end{bmatrix} \quad (\omega \leq 0.1) \quad (35)$$

The condition number at low frequency is 2.1, and the controller gives some compensation for the directionality of the plant ($\gamma(G) = 141.7$, while $\gamma(GC_\mu) = \gamma(C_\mu G) = 66.5$).

Structure of Δ_I . Note that Δ_I was assumed to be a "full" matrix in all the

calculations above. It turns out that for this particular plant (3), the same values are found for μ_{RS} and μ_{RP} also when Δ_I is assumed to be diagonal, which is a more reasonable assumption from physical consideration (there is no reason to expect that the manipulated variables will influence each other). For the DV-configuration below. It is of crucial importance to model Δ_I as a diagonal matrix and not as a full matrix.

Analysis of the DV-Configuration

The set of possible plants is given by (22) with $G = G_{DV}$ (12), but with Δ_I restricted to be diagonal. We will again consider an inverse-based and a diagonal PI controller

$$C_3(s) = \frac{k_3}{s} G_{DV}^{-1}(s) \quad (13)$$

$$C_4(s) = \frac{1+\tau s}{s} \begin{bmatrix} -0.15 & 0 \\ 0 & -7.5 \end{bmatrix} \quad (36)$$

In the simulations in Section II we studied the controller $C_3(s)$ with $k_3 = 0.7$. For this controller the Nominal Performance and Robust Stability conditions are identical to those of controller $C_1(s)$ and the LV-configuration. However, based on the simulations and other arguments presented before, μ for Robust Performance is expected to be much better. This is indeed the case, as seen from the μ -plots in Fig. 20. μ_{RP} is 0.965, which means that the performance criterion is satisfied for all possible model errors. The uncertainty block Δ_I was assumed to be diagonal. If Δ_I were full (which is not the case) the value of μ_{RP} is about 4.1. The reason for the high value in this case is that the off-diagonal elements in Δ_I introduce errors in D when V is changed.

Even lower values for μ are obtained by reducing the gain k_3 in $C_3(s)$ from 0.7 to 0.13. $k_3 = 0.13$ gives $\mu_{RP} = 0.63$. In fact, this controller seems to be very close to the μ -optimal controller for this plant, as we were not able to

reduce μ_{RP} below this value by applying the software.

With $C_4(s)$ which consists of two PI-controllers, $\mu_{RP} = 1.15$. This is almost acceptable, although the value of μ_{RP} is significantly higher than for the inversed-based controller $C_3(s)$ with $k_3 = 0.13$. Thus a decentralized controller gives acceptable performance in spite of the value of ~~0.5~~^{0.45} for the RGA which indicates strong interactions (Grosdidier, 1986)).

The potential conservativeness in using $\bar{\sigma}$ instead of μ is clearly illustrated by considering the Robust Stability test for this case (Fig. 21). Using $\mu_{\Delta_I}(H_I)$ (Δ_I diagonal) we see that the system satisfies the R.S. condition. However, by looking at $\bar{\sigma}(H_I)$ (or equivalently by computing μ with Δ_I a full matrix), we would erroneously expect the system to become unstable for very small errors on the inputs.

V. UNCERTAINTY MODELLING

In this section we will first discuss in somewhat general terms how to quantify uncertainty and then consider as an example, other sources than input uncertainty for the distillation column. In order to use the framework for analyzing systems with uncertainty outlined in Section III, we need to model the uncertainty as norm bounded perturbations. Since the uncertainty structure is very problem dependent, it is difficult to give general methods for how to do this. However, the examples given below for the distillation column should be sufficient to show that most uncertainties occurring in process control can be modelled as norm bounded perturbations.

Choosing the Right Structure

It may be very important that the correct structure is chosen for the uncertainty description, i.e., that the uncertainty is modelled as it occurs physically. We will illustrate this by considering the following two examples:

- multiplicative uncertainty at the input (Fig. 22A) or at the output of the plant (Fig. 22B)
- output uncertainty as multiplicative (Fig. 22B) or inverse multiplicative uncertainty (Fig. 22C)

Choices of Multiplicative Uncertainty. The distillation column (and any other plant) has multiplicative uncertainty at the input of the plant. Simply shifting this uncertainty to the output of the plant (and using $w_0=w_I$) will, in general, give a completely different system. As an example, for the LV-configuration using controller $C_1(s)$ we found $\mu_{RP} = 5.78$ with the uncertainty at the input of the plant, but μ_{RP} is only 0.96 if this uncertainty is shifted to the output. Recall condition (34) which showed that with input uncertainty and using an ill-conditioned controller, Robust Performance might be poor even when the R.S. and N.P. conditions were satisfied individually. We do not have this problem when the uncertainty is at the output. In this case we get a R.P. condition similar to (34) but without the condition number

$$\text{R.P.} \leq \bar{\sigma}(w_p S) + \bar{\sigma}(w_0 H) \leq 1 \quad \forall \omega$$

This illustrates that output uncertainty usually puts much less constraints on the design of the controller than input uncertainty, and for ill-conditioned plants one should be careful to model the uncertainty at the location where it is actually occurring.

Choices of Output Uncertainty. We will show below that parametric uncertainty in the time constant may be represented as inverse multiplicative uncertainty

$$(I + w_\tau \Delta_\tau)^{-1} G \tag{37}$$

Approximating it as the seemingly similar multiplicative uncertainty

$$(I + w_0 \Delta_0) G \tag{38}$$

has drastically different implications. For Robust Stability (37) imposes a

constraint on the sensitivity

$$\mu(S) \leq 1/|w_T|, S = (I+GC)^{-1} \quad (39)$$

and (38) on the complementary sensitivity

$$\mu(H) \leq 1/(|w_0|), H = GC(I+GC)^{-1} \quad (40)$$

(37) is best suited to describe pole variations while (38) is better for the modelling of zero variations. (37) cannot be used to describe uncertain high frequency dynamics. (38) cannot be used to model plants which have poles that can cross the $j\omega$ -axis.

Simplify if possible. The two examples above illustrated that it may be very important to model the uncertainties as they occur physically. However, this is not always of crucial importance, and whenever possible the uncertainty description should be simplified by lumping various uncertainties into a single perturbation. There are two reasons for this: 1) Computations are simpler, 2) Introducing too many sources of uncertainty may be very conservative since it becomes very unlikely for the "worst case" to occur in practice. In particular, the individual uncertainties may be correlated, and it may be impossible for the "worst case" to occur. This will be illustrated for the distillation column later.

Representing Nonlinearities as Uncertainty for the Distillation Column

In addition to the input uncertainty, the main source of "uncertainty" for the distillation column are nonlinearities. All the developments below are for the LV-configuration. However, because of (11) they also apply to the DV-configuration.

A simulation using the equations given in the Appendix and the input uncertainty (7) reveals that the system is unstable with the inverse-based controller $C_1(s)$ (6). Our linear analysis predicted Robust Stability, and the

reason for the discrepancy are nonlinearities which were neglected. One way of handling nonlinearities within a linear framework is to treat them as uncertainty. This is clearly not a rigorous way of handling nonlinearities, but this approach is taken in lack of anything better.

Nonlinear open loop responses to large changes (+6.2%) and a small change (0.003%) in boilup V (keeping L constant) are shown in Fig. 23. These responses may be approximated by linear first order responses:

$$V + 6.2\%: \begin{bmatrix} dy_D \\ dx_B \end{bmatrix} = \begin{bmatrix} \frac{-1.380}{73s+1} \\ \frac{-0.047}{14.5s+1} \end{bmatrix} dV \quad (41a)$$

$$V + 0.003\%: \begin{bmatrix} dy_D \\ dx_B \end{bmatrix} = \begin{bmatrix} \frac{-0.933}{267s+1} \\ \frac{1.027}{210s+1} \end{bmatrix} dV \quad (41b)$$

$$V - 6.2\%: \begin{bmatrix} dy_D \\ dx_B \end{bmatrix} = \begin{bmatrix} \frac{0.045}{46s+1} \\ \frac{1.381}{43s+1} \end{bmatrix} dV \quad (41c)$$

Note that the smallest eigenvalue of the linearized plant corresponds to a time constant of 220 min. The value $\tau = 75$ min used in the nominal model (3) represents an average value of the time constants found in the nonlinear simulations.

Time constant uncertainty. From the following simple formula for estimating the linearized time constant (Skogestad and Morari, 1986b).

$$\tau_c = \frac{N_T M_i / F}{z \ln S} \quad (42)$$

$$z = \frac{D}{F} (1-y_D) y_D + \frac{B}{F} x_B (1-x_B)$$

$$\ln S = \ln \frac{y_D (1-x_B)}{x_B (1-y_D)}$$

We find that the time constant reaches its largest value when both products have equal purity ($x_B=1-y_D=0.01$), and this explains the observation that the time constant is large for small changes in V and much smaller for large changes. In our case $N_T = 41$, $M_i/F = 0.5$ min, $z = 0.01$, $\ln S = 9.19$ and we find $\tau_C = 223$ min. The new steady state reached by increasing V by 6.2% is $y_D = 0.71403$, $x_B = 0.000602$. For this operating point we find $\ln S = 8.33$, $z = 0.102$ and $\tau_C = 24$ min. The observed variations in the time constant may be captured with the following linear model

$$G(s) = \begin{bmatrix} \frac{1}{1+\tau_D S} & 0 \\ 0 & \frac{1}{1+\tau_B S} \end{bmatrix} G(0) \quad (43a)$$

$$\tau_D = \tau(1+r_\tau \Delta\tau_D), \quad |\Delta\tau_D| < 1 \quad \forall \omega \quad (43b)$$

$$\tau_B = \tau(1+r_\tau \Delta\tau_B), \quad |\Delta\tau_B| < 1 \quad \forall \omega \quad (43c)$$

Here $\tau = 75$ min and r_τ is a constant expressing the relative uncertainty in the time constants. The scalars $\Delta\tau_D$ and $\Delta\tau_B$ are independent which allows for different values for τ_D and τ_B . Note that this model implies that both inputs always have the same time constant with respect to y_D and x_B . This is indeed what is observed when linear analysis is applied at different operating points, and this also applies to disturbances in F , z_F , etc. This pole uncertainty may be written in terms of an inverse multiplicative uncertainty at the output of the plant as shown in Fig. 24. It is fortunate that it occurs at the output since we know that the system is less sensitive to uncertainty at the output than at the input of the plant. Also note that this kind of inverse output uncertainty puts a constraint on the sensitivity function S , similar to a performance requirement. The Robust Stability test for this uncertainty alone is

$$\mu_{\Delta_{\tau}}(s) \leq 1/|w_{\tau}|, \quad w_{\tau}(s) = r_{\tau} \frac{\tau s}{\tau s + 1}$$

where Δ_{τ} is a diagonal 2x2 matrix. Clearly, we need $r_{\tau} < 1$ to satisfy this bound. It may seem strange that we have chosen the nominal value of τ to be 75 minutes, since it is clearly not possible to include even the linearized time constant (230 min) in the model (43). Recall, however, that we are trying to represent a nonlinear system. The linearized time constant only applies in a very small operating region, and as the system moves away from this steady state (maybe because of instability) the time constant will be small. It is therefore much more important to include the smallest value observed for the time constants in the approximation (43).

Gain uncertainty. We observe from (41) that the linearized gains vary tremendously with operating conditions. However, the gains are clearly correlated and it is of crucial importance to take this into account to avoid a hopelessly conservative uncertainty description. If the elements in the steady state gain matrix (3) were assumed to be independent, the gain matrix would become singular for relative errors in each of the elements exceeding (Skogestad & Morari, 1985)

$$\frac{1}{\gamma^*(G_{LV})} = \frac{1}{138.3} = 0.007 \quad (44)$$

Here $\gamma^*(G)$ is the minimized condition number

$$\gamma^*(G) = \min_{D_1, D_2} \gamma(D_1 G D_2) \quad (45)$$

D_1 and D_2 are diagonal matrices with real, positive entries. Physically we know that the distillation column will not become singular and a more structured uncertainty description is needed. Skogestad and Morari (1986c) have suggested that for small changes in D/B the variations in the steady state gains may be captured with additive uncertainty on the elements using a

single perturbation Δg . For the LV-configuration

$$G_{LV_p}(0) = G_{LV}(0) + r_g \Delta g \begin{bmatrix} 1 & -1 \\ -\frac{D}{B} & \frac{D}{B} \end{bmatrix}$$

$$= G_{LV}(0) + \begin{bmatrix} 1 \\ -\frac{D}{B} \end{bmatrix} r_g \Delta g [1 \quad -1], |\Delta g| < 1 \quad (46)$$

This model does not match our data⁽⁴⁾ too well, where large variations in D/B are observed. However, under closed loop we do not expect large changes in D/B, though the changes in L and V individually may be large and (46) with D/B = 1 will be used to represent the gain variations.

It is important to note that the additive uncertainty in (46) does not change the singular vectors \bar{v} and \underline{v} . A SVD of the perturbation matrix

$\begin{bmatrix} 1 & -1 \\ -1 & 1 \end{bmatrix}$ in (46) yields

$$\bar{v} = \begin{bmatrix} 0.707 \\ -0.707 \end{bmatrix}, \bar{u} = \begin{bmatrix} 0.707 \\ -0.707 \end{bmatrix}$$

The direction of the "input" singular vector \bar{v} is the same as that of the nominal plant (3), while the "output" singular vector \bar{u} is almost perpendicular to that of the nominal plant. This means that this source of nonlinearity is also "nice" in that it mainly changes the plant at the output. Physically this means that changes in the external flow (D and B) are always the changes with the largest effect, and this is exactly what we would expect from physical considerations, also for the nonlinear plant.

Choice of values for r_τ and r_g . There is clearly a correlation between the variations in the time constant and gains which is not captured by the proposed uncertainty description (Fig. 24). However the main effect of both these uncertainties is to change the direction of the output singular vectors, \underline{u} and

ū. None of them add RHP-zeros. In order to make computations simpler and to avoid conservative results (by neglecting the correlation between Δ_T and Δ_G), a reasonable approach may therefore be to use only one of these uncertainties to describe the effect of nonlinearity. This is the approach taken here and we choose to use the time constant uncertainty only. One reason for not choosing the gain uncertainty, is that this introduces uncertainty at steady state, which will normally not be the case since the setpoints are not changed significantly.

The trajectory taken by the plant under closed loop may be very different from the open loop responses, and open loop data such as (41) may not be appropriate to determine the value of r_T . We therefore decided to use nonlinear closed loop simulations to find an appropriate value for r_T . In particular, closed loop simulations which are at the limit to instability are convenient, since these results may easily be compared to values of μ_{RS} for the robust stability of the linear approximation. To determine the value of r_T the following procedure was used:

1. Nonlinear closed loop simulations were carried out for a large feed rate disturbance (+30%) with the inverse-based controller $C_1(s)$, $k_1 = 0.7$. The feed rate disturbance was chosen as the most difficult disturbance (Skogestad and Morari, 1986a) which would take the system furthest away from the nominal steady state. To make the elements in the matrix (9) large, the relative errors on the manipulated inputs L and V were chosen with different signs. These errors were increased until the system was at the limit to instability. The limiting values were

$$dL = 1.04 \text{ dL}, \quad dV = 0.96 \text{ dV}_C$$

2. μ_{RS} was computed for the LV-configuration with 4% input uncertainty

($w_I=0.04$) and with various values for the relative uncertainty on the time constants, r_τ . $r_\tau = 0.35$ was found to give $\mu_{RS} = 1$, i.e., correspond to a system at the limit to instability.

The value found for r_τ using this procedure is clearly not the only possible (note that no error was assume in the gains), but hopefully represents a reasonable compromise between representing all possible plants and avoiding a very conservative uncertainty description.

Effect of additional uncertainty on μ_{RS} and μ_{RP} . With the additional time constant uncertainty (43) the interconnection matrix N becomes

$$N = \begin{bmatrix} -w_I CSG & -w_I CS & w_I CS \\ w_\tau SG & w_\tau S & w_\tau (I-S) \\ w_p SG & w_p S & -w_p S \end{bmatrix} \quad (47)$$

$\mu(N)$ for R.P. (Table 2) is computed with respect to the structure $\text{diag}\{\Delta_I, \Delta_\tau, \Delta_p\}$ where Δ_I and Δ_p are "full" 2x2 matrices and Δ_τ is a diagonal 2x2 matrix. For computational convenience the matrix Δ_τ is assumed complex.

The inverse-based controller $C_1(s)$, is, of course, not robustly stable. (It was shown to be unstable with 4% input uncertainty and now there is 20%). μ_{RS} is increased from 0.53 to 4.77 by adding 35% time constant uncertainty. The μ -values for the diagonal controller, $C_2(s)$, and the " μ -optimal", $C_\mu(s)$, are seen to be only weakly influenced by adding the pole uncertainty. Robust stability is still predicted for the μ -optimal controller. This is confirmed by nonlinear simulations.

To confirm that the gain uncertainty does not significantly change these results, similar calculations were also done with the nonlinearities represented as uncertainty on the gains (Table 3). Interestingly enough, it turns out that choosing $r_g = 0.35$, $r_p = 0$ gives very similar results as $r_g = 0$,

$r_p = 0.35$, although μ increases more for low and less for high frequency with the gain uncertainty (Fig. 25). Furthermore, combination of these uncertainties were found to add up approximately in a linear fashion with respect to the value of μ . This confirms that in this case, these two sources of uncertainty (pole and gain uncertainty) have a very similar effect on the plant, and that for computational simplicity we need to use only one of them. Similar results are found for the DV-configuration (Table 3), although the pole uncertainty is found to be worse than the gain uncertainty.

The conclusions with respect to the effect of the nonlinearities for the distillation column are

1. The main effect of the nonlinearities is to change the "directions" at the output of the plant.
2. Representing this effect by uncertainty in the time constant seems to be a good approach.
3. Since output uncertainty may be thought of as a output "disturbance", controllers which were found to give good Robust Performance in Section IV, are not affected very much by these nonlinearities.

VI. RELATIONSHIP TO THE RGA

Because of the extensive use of the RGA as a tool for evaluating control configurations for distillation column (Shinskey, 1984), we will briefly discuss some relationships between the RGA and uncertainty for 2x2 systems.

As defined, the RGA is primarily a tool for investigating the use of decentralized control. Each element in the RGA is defined as the open loop gain divided by the gain between the same two variables when all other loops are under "perfect" control

$$\lambda_{ij} = \frac{(\partial y_i / \partial u_j)_{u_{k \neq j}}}{(\partial y_i / \partial u_j)_{u_{k \neq j}}} = \frac{\text{Gain all other loops open}}{\text{Gain all other loops closed}} \quad (48)$$

For 2x2 plants

$$\text{RGA} = \begin{bmatrix} \lambda_{11} & 1-\lambda_{11} \\ 1-\lambda_{11} & \lambda_{11} \end{bmatrix}, \lambda_{11} = \frac{1}{1-A}, A = \frac{g_{12}g_{21}}{g_{11}g_{22}} \quad (49)$$

The RGA therefore tells something about how the system is changed as loops are changed from being "open" to being "closed". Such changes are frequently done in the process industry, for example due to failures in measurements or actuators, and it is clearly desirable to be able to do this without upsetting the rest of the system or having to retune the controllers. It is therefore desirable to choose pairings of inputs and outputs which have λ_{ij} close to one. Pairing of variables with negative values of λ_{ij} is not desirable since the loop gains in this case may change sign as we open or close other loops. Consequently, from the definition of RGA we can clearly see some useful properties of this measure. However, the RGA is used as a measure of control quality in a much wider sense than suggested by its definition. In particular, large elements in the RGA are suggested to imply a plant which is fundamentally difficult to control. We will look at this in the context of uncertainty.

Result 1. Relative Uncertainty (2x2) (Skogestad & Morari, 1985)

Let the uncertainty be given in terms of equal relative errors r on each of the individual elements

$$G_p = \begin{bmatrix} g_{11}(1+r\Delta_{11}) & g_{12}(1+r\Delta_{12}) \\ g_{21}(1+r\Delta_{21}) & g_{22}(1+r\Delta_{22}) \end{bmatrix}, |\Delta_{ij}| < 1 \quad (50)$$

The plant will remain nonsingular for any real perturbations $|\Delta_{ij}| < 1$ if and only if

$$r < \frac{1}{\gamma^*(G)} \quad (51)$$

which is satisfied if

$$r < \frac{1}{\|RGA\|_1}, \quad \|RGA\|_1 = 2|\lambda_{11}| + 2|1-\lambda_{11}| \quad (52)$$

The result in (51) has already been used in (44). Note in particular that it is impossible to have integral control for a plant which may become singular at steady state. Consequently, if there are large values in the RGA and $\|RGA\|_1$ is large, we can allow only very small uncertainties in the elements without having control problems. The main restriction with this result is the assumption made about the independent uncertainty on the elements. For distillation columns, even though $\|RGA\|_1$ is large and the elements in G may vary widely with operating conditions, the elements are strongly correlated, and it can be shown that the plant will never become singular. For distillation column control, Result 1 does therefore not "explain" why plants with large values of the RGA are difficult to control. However, since uncertainty on the manipulated inputs is always present, and since performance is usually measured at the output of the plant, the following result is of more interest.

Result 2. Input Uncertainty (2x2)

Let Δ_1 and Δ_2 represent the magnitude of the relative uncertainty of each of the manipulated inputs. The matrix $G\Delta G^{-1}$ (Eq. 8) becomes

$$G\Delta G^{-1} = \begin{bmatrix} \lambda_{11}\Delta_1 + \lambda_{12}\Delta_2 & -\lambda_{11} \frac{g_{12}}{g_{22}} (\Delta_1 - \Delta_2) \\ \lambda_{11} \frac{g_{21}}{g_{11}} (\Delta_1 - \Delta_2) & \lambda_{12}\Delta_1 + \lambda_{11}\Delta_2 \end{bmatrix} \quad (53)$$

The matrix $G\Delta G^{-1}$ arises when we have input uncertainty and use a inverse-based controller. As argued before, large elements in the matrix $G\Delta G^{-1}$ implies that

the system is sensitive to this uncertainty. The following is clear from (53)

1. Large values of λ_{11} always imply poor performance since the diagonal elements will be large in magnitude.
2. However, performance can be bad even if λ_{11} is small. This will happen if g_{12}/g_{22} or g_{21}/g_{11} is large. One example is a triangular plant which always has $\lambda_{11} = 1$, but which will be sensitive to input uncertainty if the off-diagonal element is large.

If an inverse based controller is not used, the arguments above do not hold. However, in this case the response will be strongly dependent on the disturbance directions. In conclusion, Eq. (53) at least gives one reason for why distillation columns with large elements in the RGA are fundamentally difficult to control.

References

- Doyle, J. C. and G. Stein, Multivariable Feedback Design: Concepts for a Classical/Modern Synthesis, IEEE Trans. Automat. Contr., AC-26, 1, 4-16 (1981).
- Doyle, J. C., Analysis of Feedback Systems with Structured Uncertainties, Proc. IEE, 129, D(6), 242-247 (1982).
- Doyle, J. C., Structured Uncertainty in Control System Design, 24th CDC, Ft. Lauderdale, FL (1985).
- Doyle, J. C., lectures and personal communications, Caltech (1986).
- Grosdidier, P. and M. Morari, Interaction Measures for Systems Under Decentralized Control, Automatica, 22, 3, 309-319 (1986).
- Morari and J. Doyle, A Unifying Framework for Control System Design Under Uncertainty and its Implication for Chemical Process Control, CPC 1986, Asilomar, CA, Jan. (1986).
- Moczek, J. S., R. E. Otto and T. J. Williams, Approximate Models for the Dynamic Response of Large Distillation Columns, Chem. Eng. Progr. Symp. Ser., No. 61, 136-146 (1965).
- Shinskey, F. G., Distillation Control, McGraw-Hill, 1984.
- Skogestad, S. and M. Morari, Design of Resilient Processing Systems. Effect of Model Uncertainty on Dynamic Resilience (submitted to Chem. Eng. Sci. (1985).
- Skogestad, S. and M. Morari, Effect of Disturbance Directions on Closed Loop Performance, submitted to Ind. Eng. Chem. Process Des. Dev. (1986a).
- Skogestad, S. and M. Morari, Shortcut Models for the Dynamic Behavior of Distillation Column, in progress (1986b).
- Skogestad, S. and M. Morari, Nonlinearity and Uncertainty in the Steady State Gain Matrix for Distillation Columns, in progress (1986c).
- Stein, G., Beyond Singular Values and Loop Shapes, 24th CDC, Ft. Lauderdale, FL (1985).

Appendix. Simplified nonlinear dynamical model of distillation column with total condenser.

Assumptions:

- Constant molar flows
 - No vapor holdup (immediate vapor response, $dV_{top} = dV_{btm}$)
 - Liquid holdup M_i constant (immediate liquid response, $dL_{top} = dL_{btm}$)
 - Vapor Liquid Equilibrium (VLE) and perfect mixing on each stage
 - Perfect level control in accumulator and column base, pressure constant
- N - no. of equilibrium (theoretical) stages including the reboiler
 $N_T = N + 1$ - total no. of stages including total condenser
 N_F - feed stage location

Material balance describing change in holdup of light component on each tray:
 $i = 2, N$ ($i \neq N_F, i \neq N_T$):

$$M_i \dot{x}_i = L_{i+1} x_{i+1} + V_{i-1} y_{i-1} - L_i x_i - V_i y_i$$

Above feed location, $i = N_F + 1$

$$M_i \dot{x}_i = L_{i+1} x_{i+1} + V_{i-1} y_{i-1} - L_i x_i - V_i y_i + F_V y_F$$

Below feed location, $i = N_F$

$$M_i \dot{x}_i = L_{i+1} x_{i+1} + V_{i-1} y_{i-1} - L_i x_i - V_i y_i + F_L x_F$$

Reboiler, $i = 1$

$$M_B \dot{x}_1 = L_{i+1} x_{i+1} - V_i y_i - B x_1, \quad x_B = x_1$$

Total condenser, $i = N_T$

$$M_D \dot{x}_{N_T} = V_{i-1} y_{i-1} - L_i x_i - D x_{N_T}, \quad y_D = x_{N_T}$$

VLE on each tray

$$y_i = \frac{\alpha x_i}{1 + (\alpha - 1) x_i}, \quad i = 1, N$$

Flow rates

$$i > N_F \text{ (above feed):} \quad L_i = L, \quad V_i = V + F_V$$

$$i \leq N_F \text{ (below feed):} \quad L_i = L + F_L, \quad V_i = V$$

$$F_L = q_F F, \quad F_V = F - F_L$$

$$D = V_{N_T} - L_{N_T} = V + F_V - L \text{ (accumulator holdup constant)}$$

$$B = L_2 - V_1 = L + F_L - V \text{ (column base holdup constant)}$$

Compositions x_F and y_F are found by solving the flash equations for the feed

$$Fz_F = F_Lx_F + F_Vy_F$$

$$y_F = \frac{\alpha x_F}{1 + (\alpha - 1)x_F}$$

Binary separation, constant molar flows

Relative volatility	$\alpha = 1.5$
No. of theoretical trays	$N = \frac{4}{50}$
Feed tray location	$N_F = 21$
Feed rate and composition	$F = 1 \text{ kmol/min}, z_F = 0.5$
Fraction of liquid in feed	$q_F = 1.0$
Product compositions	$y_D = 0.99, x_B = 0.01$
Product rates	$D = B = 0.5 \text{ kmol/min}$
Tray holdup	$M_i = 0.5 \text{ kmol}, i = 2, 40$
Accumulator and column base holdup	$M_D = 32.1 \text{ kmol}, M_B = 11.1 \text{ kmol}$

Computed at steady state from nonlinear model (Appendix)

Reflux rate	$L = 2.71 \text{ kmol/min} (1.39 \text{ L}_{\text{min}})$
Boilup rate	$V = 3.21 \text{ kmol/min}$
Linearized steady state gains	

$$\begin{bmatrix} dy_D \\ dx_B \end{bmatrix} = \begin{bmatrix} 0.878 & -0.864 \\ 1.082 & -1.096 \end{bmatrix} \begin{bmatrix} dL \\ dV \end{bmatrix} + \begin{bmatrix} 0.394 \\ 0.586 \end{bmatrix} dF + \begin{bmatrix} 0.881 \\ 1.119 \end{bmatrix} dz_F$$

Table 1. Data for distillation column example.

Input Uncertainty, $w_I = 0.2 \frac{5s+1}{0.5s+1}$

	$r_T=r_g=0$			$r_T=0.35$		$r_g=0.35$	
	μ_{NP}	μ_{RS}	μ_{RP}	μ_{RS}	μ_{RP}	μ_{RS}	μ_{RP}
LV-configuration							
Inverse-Controller, $C_1(s), k_1=0.7$	0.50	0.53	5.78	4.77	7.50	4.83	7.53
Diagonal PI, $C_2(s), k_2=2.4$	1.50	1.39	1.70	1.61	1.91	1.47	1.82
Optimal Inverse, $C_1(s), k_1 = 0.14$	0.50	0.20	3.29	2.60	4.18	2.62	4.19
" μ -optimal", $C_\mu(s)$	0.79	0.72	1.06	0.99	1.29	0.87	1.24
DV-configuration							
Inverse-controller, $C_3(s), k_3=0.7$	0.50	0.53	0.97	0.83	1.18	0.53	1.07
Diagonal PI, $C_4(s)$	0.81	0.37	1.14	0.85	1.61	0.61	1.45
Optimal Inverse, $C_3(s), k_3=0.13$	0.50	0.20	0.63	0.47	0.81	0.20	0.73

Table 2. Values of μ_{NP} , μ_{RS} and μ_{RP} for distillation column with diagonal input uncertainty, and effect on μ_{RS} and μ_{RP} (μ_{NP} is unchanged) by adding time constant uncertainty (r_T) and gain uncertainty (r_g).

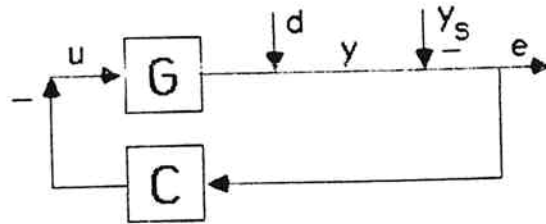


Figure 1. Classical linear feedback structure with error e as input to the controller. d represents the effect of the disturbance on the outputs y .

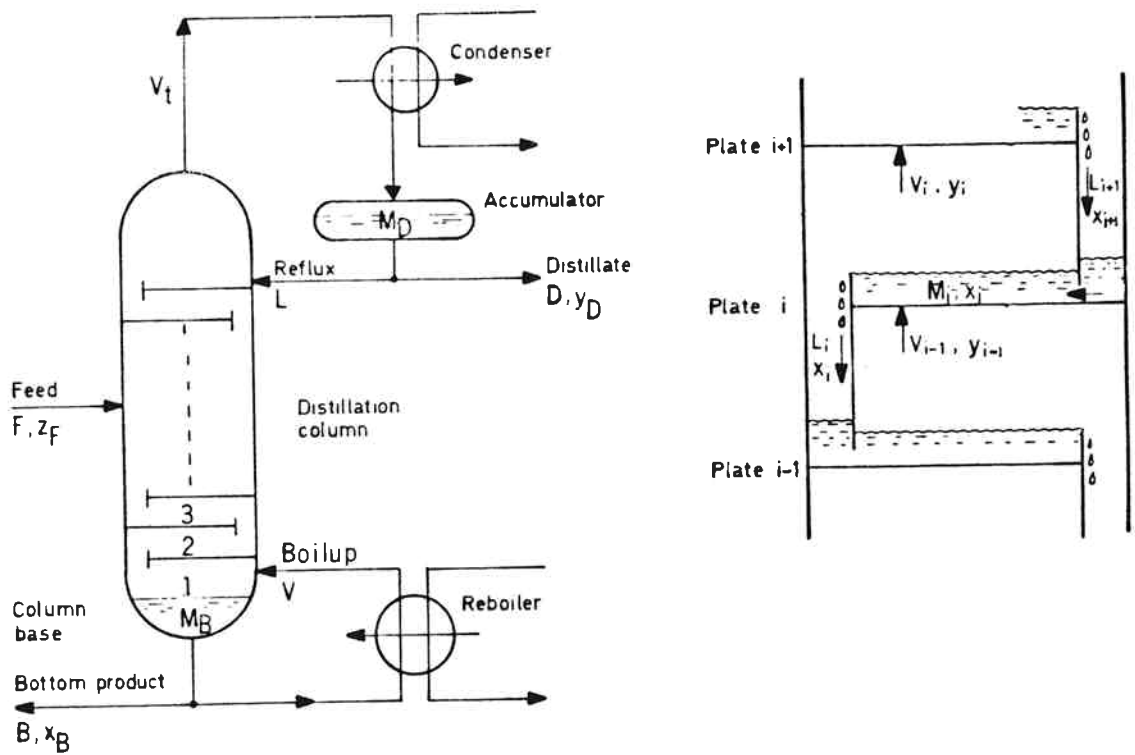


Figure 2. Two product distillation column with single feed and total condenser. Details are shown of the flows and holdups on a plate.

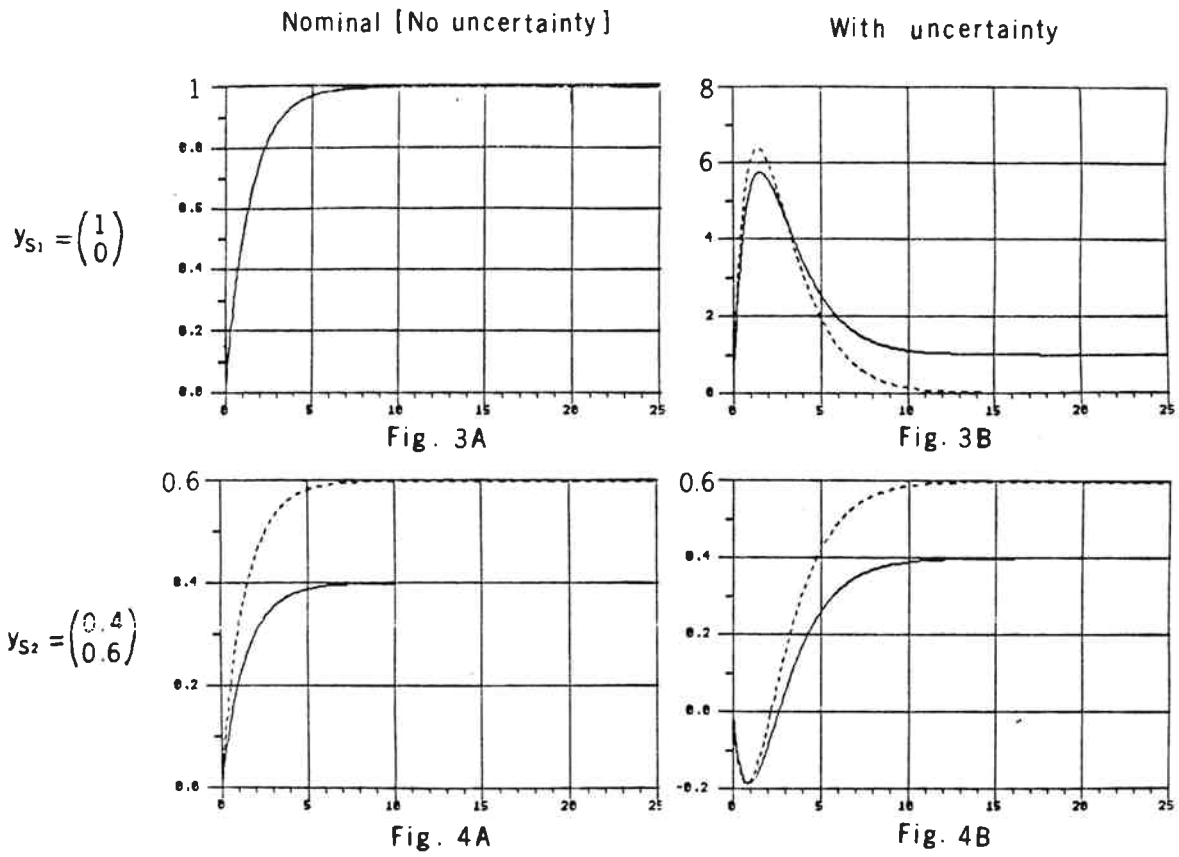


Figure 3 and 4. Closed loop responses Δy_D and Δx_B with inverse-based controller, $C_1(s)$, $k_1 = 0.7$ (time in minutes).

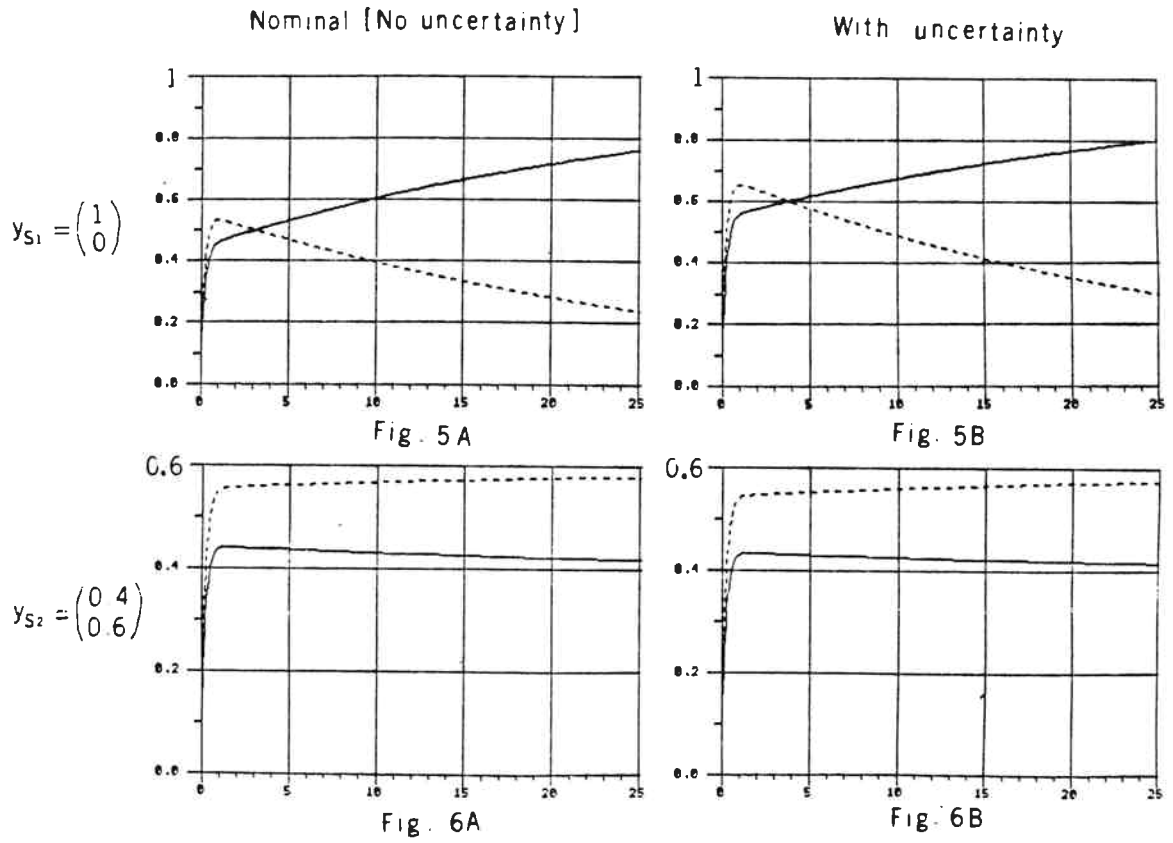


Figure 5 and 6. Closed loop responses Δy_D and Δx_B with diagonal controller, $C_2(s)$, $k_2 = 2.4$ (time in minutes).

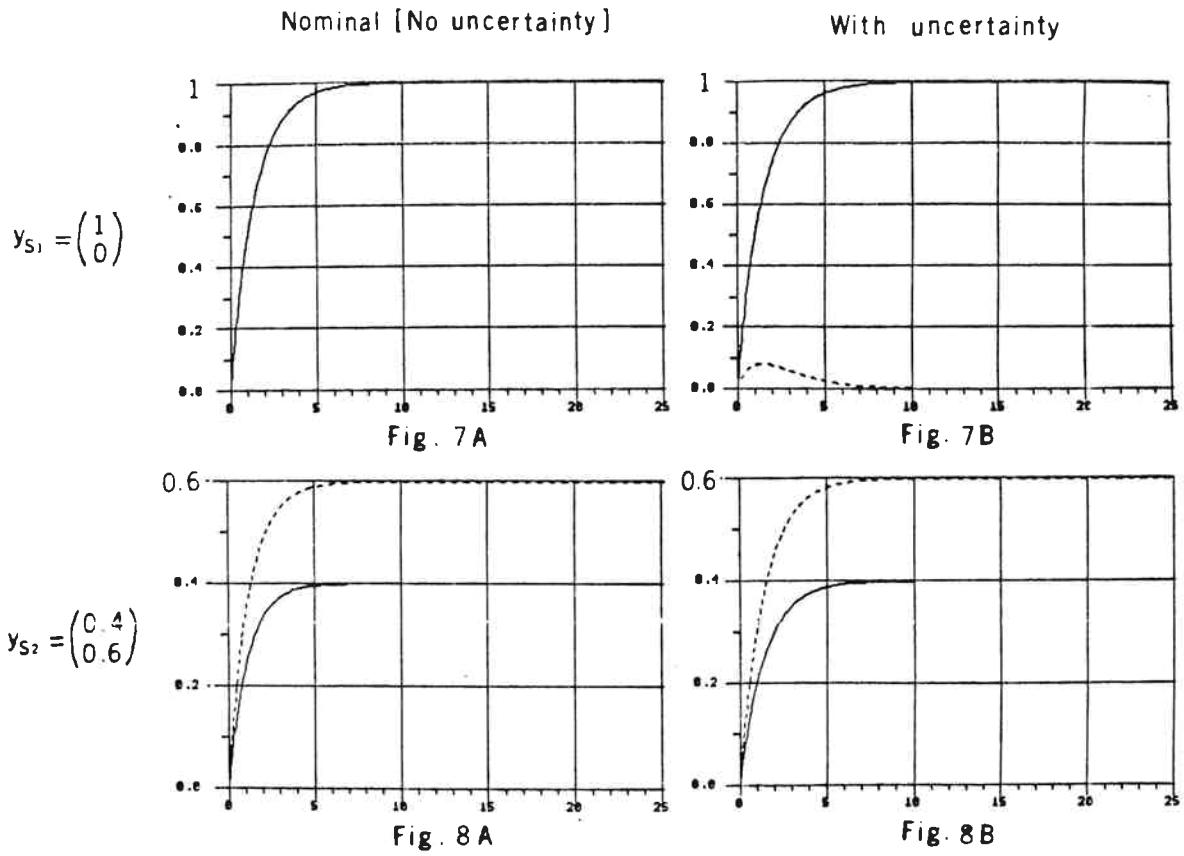


Figure 7 and 8. DV-configuration. Closed loop responses Δy_D and Δx_B with inverse-based controller, $C_3(s)$, $k_3 = 0.7$ (time in minutes).

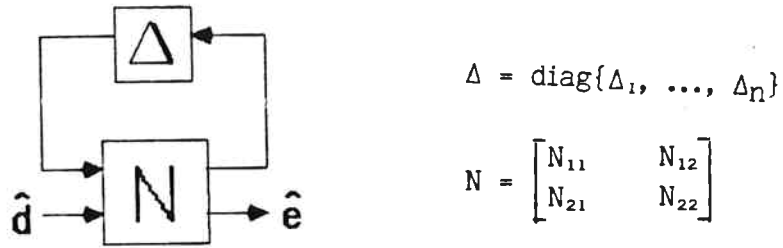


Figure 9. General representation of system with uncertainty Δ . \hat{d} represents weighted external inputs, \hat{e} represents weighted errors.

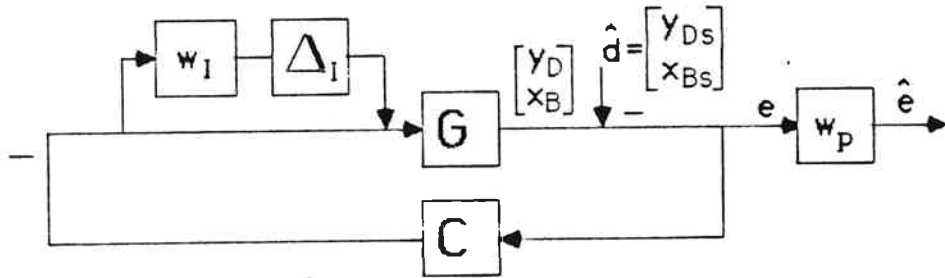


Figure 10. Block diagram of system with input uncertainty and with setpoints as external inputs. Rearranging this system to fit Fig. 9 gives N as in Eq. (27):

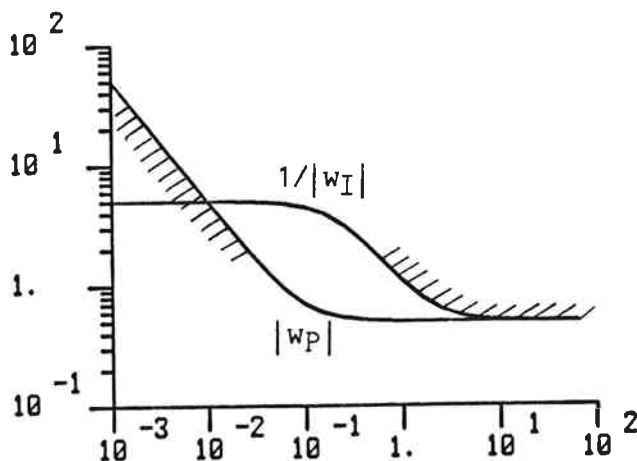


Figure 11. Multivariable loop shaping. For Nominal Performance, $\bar{\sigma}(GC)$ must lie above $|w_P|$ at low frequencies. For Robust Stability with input uncertainty, $\bar{\sigma}(CG)$ must lie below $1/|w_I|$ at high frequencies.

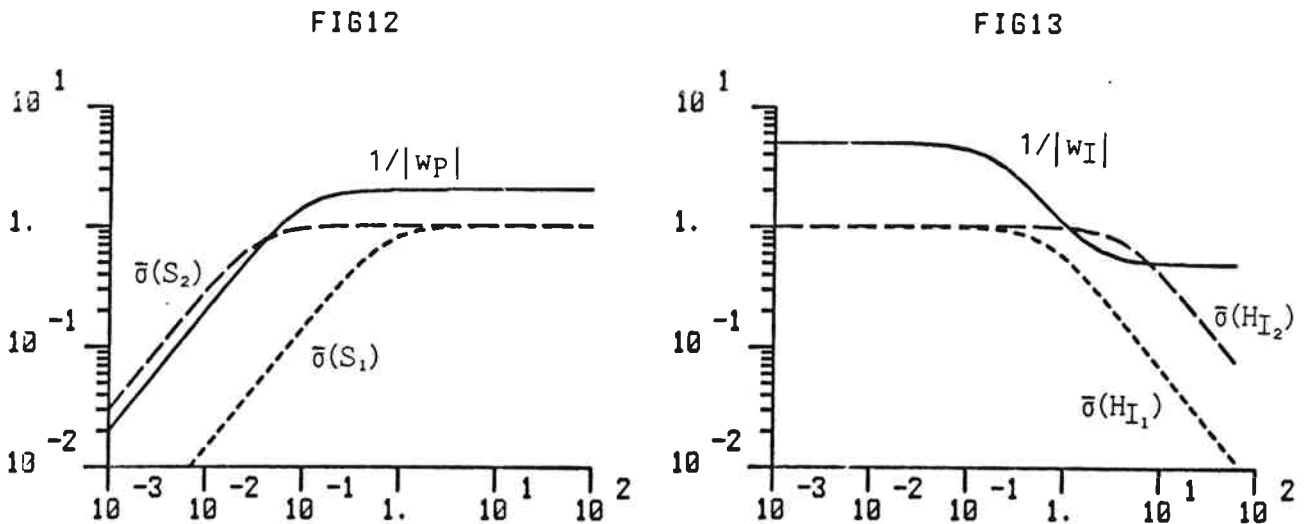


Figure 12. The inverse-based controller, $C_1(s)$, $k_1 = 0.7$ has much better Nominal Performance than required by the condition $\bar{\sigma}(S) < 1/|w_p|$, $\forall \omega$. The diagonal controller, $C_2(s)$, $k_2 = 2.4$, does not satisfy the N.P. condition at low frequency.

Figure 13. The inverse-based controller, $C_1(s)$, $k_1 = 0.7$ is guaranteed Robust Stability since $\bar{\sigma}(H_I) < 1/|w_I|$, $\forall \omega$. The diagonal controller, $C_2(s)$, $k_2 = 2.4$ will give an unstable system for some of the plants defined by (22), since the R.S condition is not satisfied at all frequencies.

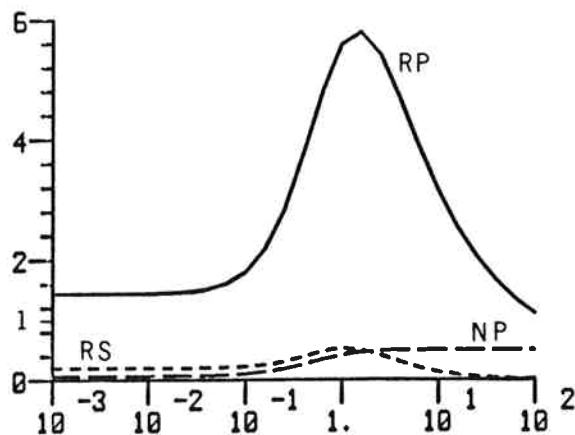


Figure 14. μ -plots for inverse-based controller, $C_1(s)$, $k_1 = 0.7$. The system has very good performance when the plant is equal to the plant model, and is guaranteed stability for all plants given by (22), but robust performance is poor.

FIG15

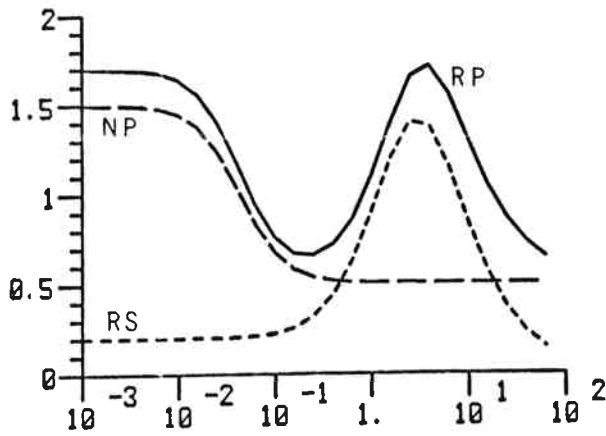


FIG16

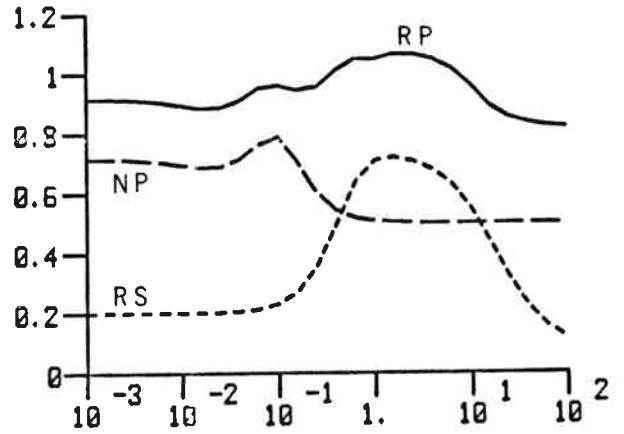


Figure 15. μ -plots for diagonal controller, $C_2(s)$, $k_2 = 2.4$.

Figure 16. μ -plots for "mu-optimal" controller, $C_\mu(s)$.

Nominal [No uncertainty]

With uncertainty

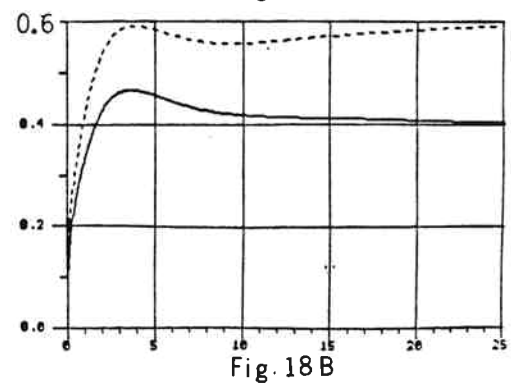
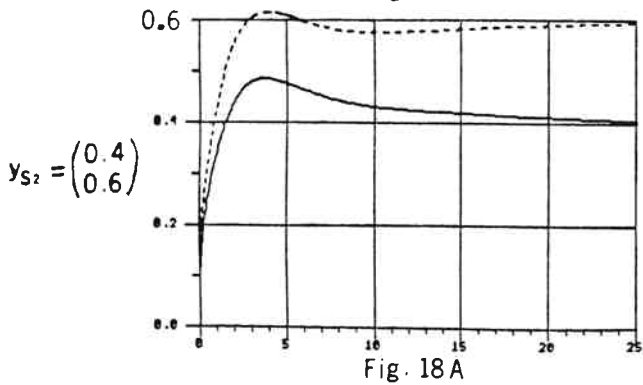
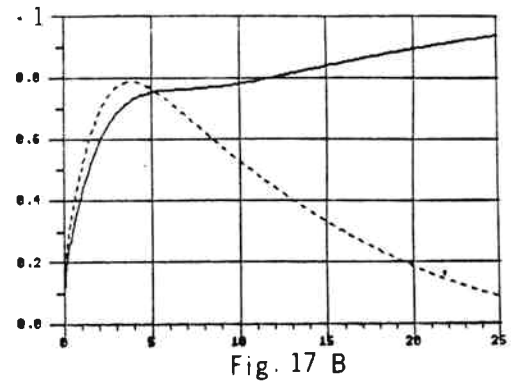
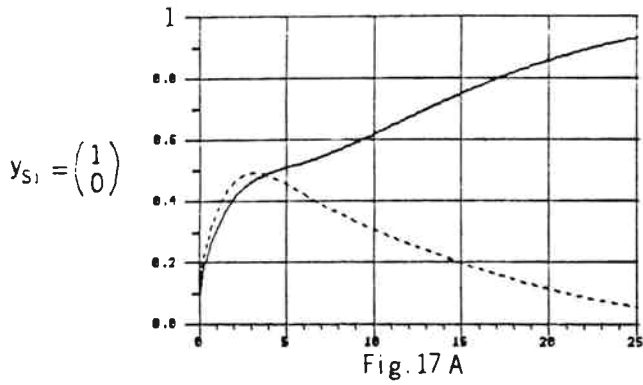


Figure 17 and 18. Closed-loop responses Δy_D and Δx_B with "mu-optimal" controller, $C_\mu(s)$ (time in minutes).

$$A = \begin{bmatrix} -1.002E-07 & 0.000E+00 & 0.000E+00 & 0.000E+00 & 0.000E+00 & 0.000E+00 \\ 0.000E+00 & -3.272E-06 & 0.000E+00 & 0.000E+00 & 0.000E+00 & 0.000E+00 \\ 0.000E+00 & 0.000E+00 & -1.510E-01 & 0.000E+00 & 0.000E+00 & 0.000E+00 \\ 0.000E+00 & 0.000E+00 & 0.000E+00 & -9.032E+00 & 0.000E+00 & 0.000E+00 \\ 0.000E+00 & 0.000E+00 & 0.000E+00 & 0.000E+00 & -5.838E+02 & 0.000E+00 \\ 0.000E+00 & 0.000E+00 & 0.000E+00 & 0.000E+00 & 0.000E+00 & -5.868E+02 \end{bmatrix}$$

$$B = \begin{bmatrix} -6.513E+01 & -9.009E+01 \\ 7.224E+01 & 9.031E+01 \\ 5.492E+00 & -4.394E+00 \\ -9.086E+01 & -1.136E+02 \\ 1.867E+03 & -1.494E+03 \\ 6.722E+02 & 8.403E+02 \end{bmatrix}$$

$$C = \begin{bmatrix} 6.564E-01 & 7.171E-01 & 4.949E+00 & 5.033E+00 & -1.691E+03 & -3.112E+02 \\ 6.555E-01 & 5.425E-01 & 4.941E+00 & -5.040E+00 & -1.689E+03 & 3.116E+02 \end{bmatrix}$$

$$D = \begin{bmatrix} 5.866E+03 & -3.616E+03 \\ 5.002E+03 & -4.878E+03 \end{bmatrix}$$

Figure 19. State space realization of "μ-optimal" controller, $C_{\mu}(s) = C(sI-A)^{-1}B + D$.

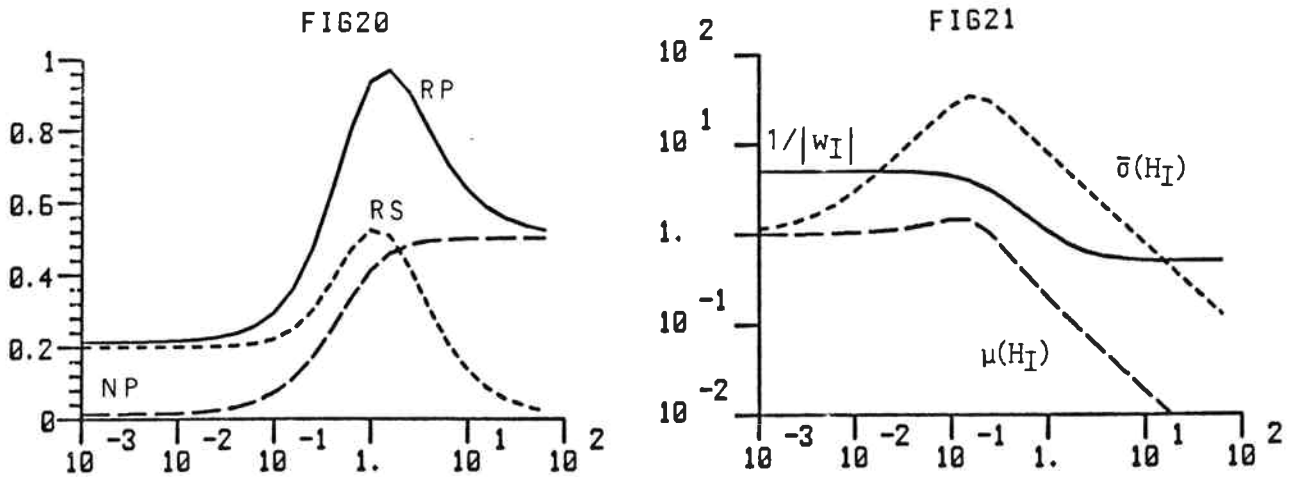


Figure 20. DV-configuration. μ -plots for inverse-based controller, $C_3(s)$, $k_3 = 0.7$.

Figure 21. DV-configuration. Robust Stability for controller $C_4(s)$. Using $\bar{\sigma}(H_I)$ instead of $\mu(H_I)$ will be very conservative in this case, and one would mistakenly conclude that the system does not satisfy the R.S. condition $\mu(H_I) < 1/|w_I|$.

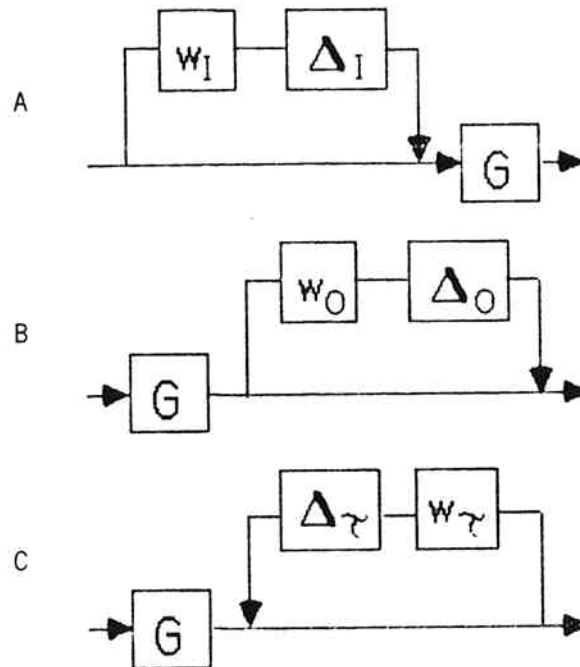


Figure 22. Three common uncertainty representations. (A) Input multiplicative uncertainty; (B) Output multiplicative uncertainty; (C) Output inverse multiplicative uncertainty.

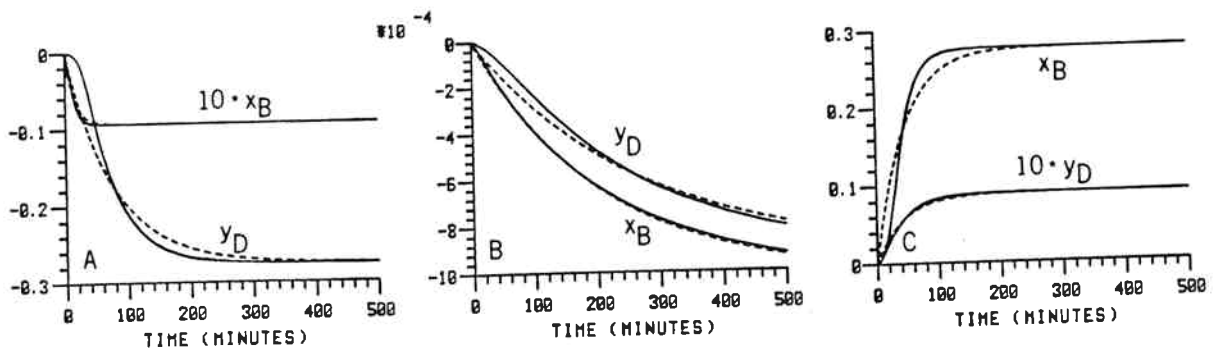


Figure 23. (—) Nonlinear open loop responses Δy_D and Δx_B for changes in boilup V (reflux L constant). (---) Approximation with linear first order response (Eq. 41).
 A: $V + 6.2\%$, B: $V + 0.003\%$, C: $V - 6.2\%$.

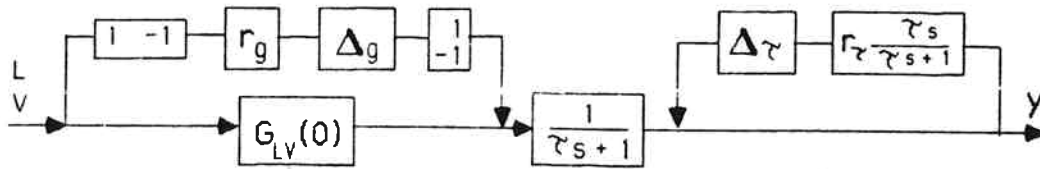


Figure 24. . Block diagram representation of gain uncertainty and time constant uncertainty.

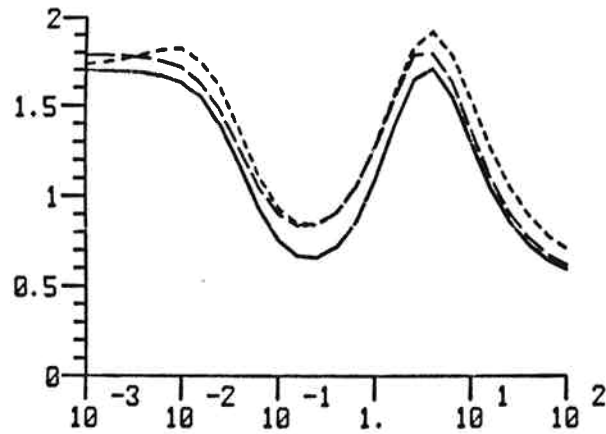


Figure 25. μ -plots for R.P. for diagonal controller, $C_2(s)$, $k_2 = 0.7$. The addition of gain or time constant uncertainty is seen to have a similar and not too significant effect on the value of μ .
 (—): $r_\tau = r_g = 0$, (---): $r_g = 0.35$, (-·-·-): $r_\tau = 0.35$

